Chemical Engineering Journal 372 (2019) 496–508

Contents lists available at ScienceDirect

Chemical Engineering Journal

journal homepage: www.elsevier.com/locate/cej

Robust multifunctional microcapsules with antibacterial and anticorrosion features

Yong Bing Chong[a], Dawei Sun[b,c], Xin Zhang[d], Chee Yoon Yue[a,*], Jinglei Yang[b,*]

[a] School of Mechanical and Aerospace Engineering, Nanyang Technological University, Singapore
[b] Department of Mechanical and Aerospace Engineering, Hong Kong University of Science and Technology, Hong Kong SAR, China
[c] Beijing University of Technology, College of Materials Science and Engineering, Beijing, China
[d] School of Civil and Environmental Engineering, Nanyang Technological University, Singapore

HIGHLIGHTS

- Encapsulation of 8-HQ by dissolving in clove oil is achieved through in situ polymerization.
- The final PMF shell is thick and robust mechanically.
- Multifunctional coatings present good antibacterial and anticorrosion properties.

ARTICLE INFO

Keywords:
Microcapsules
Clove oil
8-HQ
Antibacterial
Anticorrosion
Multifunctional

ABSTRACT

Corrosion and biofouling are two common unsolved problems in the marine industry, urging the need of innovative solutions to tackle both problems simultaneously. Herein, the fabrication of multifunctional microcapsules containing 8-hydroxyquinoline (8-HQ) as the corrosion inhibitors and clove oil as the natural antimicrobial compound is described to resolve both corrosion and biofouling problems simultaneously. Microcapsules containing 8-HQ and clove oil, featuring good mechanical properties, anticorrosion, and antibacterial properties, were successfully synthesized through in-situ polymerization of melamine-formaldehyde polymer. The fabricated microcapsules show antibacterial properties against *Escherichia coli*, *Vibrio coralliilyticus* and *E. aestuarii*, as revealed from the standard ASTM E2315 time-kill test. Multifunctional coatings with both antibacterial and anticorrosion features were fabricated by incorporating the fabricated microcapsules both onto and into the epoxy coatings. According to the zone inhibition test, the microcapsules-based multifunctional coating possesses antibacterial properties against the seawater bacteria. Manually scratched microcapsules-based multifunctional coatings possess anticorrosion properties, due to the formation of corrosion inhibition layer resulted from the reaction between the released 8-HQ compound and the mild steel substrate. Additionally, after 30 days of immersion in the salt water, the microcapsules-based coatings still possess anticorrosion properties by forming corrosion inhibition layer at the scratched region.

1. Introduction

Corrosion remains as an unsolved challenging problem, which has caused huge economic losses annually, especially for the marine industry due to the corrosive environment. The use of corrosion inhibitors is one of the most traditional approaches to prevent corrosion attack through adsorption of ions and molecules onto metal surface, to minimize the reaction between metal and corrosive medium [1–3]. According to previous research, corrosion inhibitors are usually organic compounds with π bonds and heteroatoms (P, N, S and O) [4]. The use of organic compound corrosion inhibitors for steels includes acetylenic alcohols, aromatic aldehydes, benzimidazoles, nitrogen-containing heterocycles, quinoline derivatives, quaternary salts and etc [1,5–7]. Despite their great anticorrosion properties, undesirable interaction of the corrosion inhibitors with the coating matrix often contributes to the reduction of inhibition efficiency and weakening of coating properties. Hence, microencapsulation of corrosion inhibitors is relatively important to prevent this undesirable interaction while maintaining effective corrosion inhibition properties.

8-hydroxyquinoline (8-HQ) is one of the most commonly used

* Corresponding authors.
E-mail addresses: mcyyue@ntu.edu.sg (C.Y. Yue), maeyang@ust.hk (J. Yang).

https://doi.org/10.1016/j.cej.2019.04.139
Received 5 November 2018; Received in revised form 12 April 2019; Accepted 20 April 2019
Available online 22 April 2019
1385-8947/

corrosion inhibitors for different types of substrates including mild steel, aluminum and magnesium alloys [8–11]. Recent studies have shown the encapsulation of 8-HQ using ceria [12] and titania nanocontainers [13] to exhibit anticorrosion effect against AA2024. Additionally, polyurea microcapsules containing 8-HQ was also synthesized through interfacial polymerization between toluene diisocyanate (TDI) and PAMAM dendrimer [14]. While the encapsulation of 8-HQ was successful, the mechanical properties of the microcapsules requires improvement to withstand harsh industrial processing conditions and the agglomeration problem of the microcapsules should be eliminated. Moreover, the use of organic solvent such as toluene and xylene to dissolve 8-HQ is undesirable as the release of these organic solvents can pose potential environmental hazards and health problems [15,16]. To overcome these shortcomings, better encapsulation process and alternative environmental friendly solvent to dissolve 8-HQ are thus essential.

Apart from corrosion, biofouling is another challenging problem and several innovative antibacterial or antifouling coatings have been proposed in recent years [17–21]. Today, most antifouling coatings involve the use of biocides such as Irgarol, copper pyrithione and 4,5-Dichloro-2-n-octyl-4-isothiazolin-3-one (DCOIT), after the official ban of tributyltin (TBT) compound due to its toxicity [22]. However, the toxicity of these biocides was also revealed in recent studies [23–25], urging the need of alternative solutions which are more environmental friendly. Notably, the use of natural compounds such as essential oils can potentially contribute to a more environmental friendly option to tackle these problems. Essential oils such as clove, thyme, rosemary and lemongrass oils have shown antibacterial effect against a wide range of bacterial strains [26,27]. For instance, recent studies have shown excellent antibacterial effect of clove oil against different types of marine bacteria, indicating their potential in tackling the marine fouling problem [28]. Despite the good antibacterial properties of these essential oils, their volatility and chemical instability remains a challenging problem in the translation into practical uses, urging the need of microencapsulation to isolate them from the surrounding environment [29,30].

Based on the needs of encapsulation for both corrosion inhibitors and essential oils, innovative idea of fabricating multifunctional microcapsules combining both anticorrosion and antibacterial purposes was proposed. In this study, 8-HQ dissolved in clove oil is encapsulated successfully through in-situ polymerization technique to fabricate multifunctional microcapsules with both antibacterial and anticorrosion features. The fabricated microcapsules have shown good antibacterial properties against *E. coli* and *V. coralliilyticus* through the ASTM time-kill test. Additionally, multifunctional coating containing the fabricated microcapsules possesses antibacterial properties against the seawater bacteria, indicating great potential to solve biofouling problem. Through accelerated anticorrosion test, the scratched multifunctional coating has shown good anticorrosion behavior through adsorption of corrosion inhibition layer on the metal surface which retards corrosion attack to the exposed steel substrate.

2. Materials and methods

2.1. Materials

Melamine, 37 wt% formaldehyde solution, clove oil, 8-hydroxyquinoline (8-HQ), sodium dodecyl benzenesulfonate (SDBS), polyvinyl alcohol (PVA), sodium chloride (NaCl), sodium hydroxide (NaOH) and acetic acid were purchased from Sigma Aldrich. Epolam 5015 and hardener 5015 used as epoxy matrix were supplied by Axson. All the chemicals were used without any further purification.

2.2. Synthesis of microcapsules containing 8-hydroxyquinoline and clove oil

8-hydroxyquinoline (8-HQ) dissolved in clove oil was successfully encapsulated using in-situ polymerization of melamine -formaldehyde as the shell material [31]. Mixture of 3.75 g melamine and 9.5 g of 37 wt% formaldehyde solution was prepared and the pH value of the final mixture was adjusted to 8.5–9.0 using NaOH solution. The pre-polymer solution of melamine-formaldehyde was then put into a water bath of 70 °C under magnetic stirring for 1 h on a programmable hotplate. For the preparation of the surfactant solution, 0.6 g of sodium dodecylbenzenesulfonate (SDBS) and 0.09 g of polyvinyl alcohol (PVA) were mixed thoroughly in 30 ml of DI water and placed into a water bath of 55 °C on a programmable hotplate. The prepared pre-polymer solution of melamine-formaldehyde was then added into the above surfactant solution and allowed to settle for a few minutes. The core material of 20% 8-HQ dissolved in clove oil solution was prepared by mixing 2.125 g of 8-HQ compound with 8.5 g of clove oil. Strong mechanical vortex mixing was employed to ensure thorough dissolve of 8-HQ compound in the liquid clove oil. Under an agitation rate of 200 rpm, the core material was added drop wise into the system and the ensuing emulsification was allowed to take place for 1 h. After stabilizing the emulsification, the pH value of the system was slowly tuned to around 4.3 by adding 10 ml of 1 M acetic acid at a very slow rate of 0.1 ml/min using the syringe pump system. Subsequently, the system was left to react for another 3 h at 55 °C. The obtained suspension of microcapsules slurry was rinsed with DI water for 5 times. Finally, the collected microcapsules were air dried for 12 h and sieved to remove debris before further analysis and characterizations.

2.3. Determination of microcapsules content

Fourier Transform infrared (FTIR) spectra were acquired using FTIR spectrometer to study on the chemical structure of the microcapsules. Different testing samples were prepared by grinding with potassium bromide (KBr). Subsequently, infrared light was transmitted through the samples to obtain different FTIR spectra. To confirm successful encapsulation of 8-HQ dissolved in clove oil, the FTIR spectra of different samples including clove oil, 8-HQ, pure mixture of clove oil and 8-HQ and core material were obtained and examined carefully. Additionally, the FTIR spectrum of the scrapped corrosion inhibition layer formed at the scratched region of the multifunctional coating exposed to corrosion test, was also acquired using similar procedure.

2.4. Core fraction

The core fraction of the fabricated microcapsules was determined by the extraction method with the use of ethanol as the extracting solvent. 0.1 g of the fabricated microcapsules (W_1) was weighed and poured into a folded filter paper. Subsequently, the microcapsules were squeezed firmly to completely release the encapsulated core material – 8-HQ and clove oil. The mixture of 8-HQ and clove oil was then extracted from the broken microcapsules using ethanol. To ensure complete extraction, the extraction process was repeated 5 times and the remaining weight (W_2) of shell material was measured carefully. The extraction test was conducted 3–5 times to determine the average value. Additionally, the core contents of the fabricated microcapsules after different storage period in the glass vial were also measured using the above procedure. The calculation of core content is based on the equation below:

$$Core\ content\ (\%) = \frac{W_1 - W_2}{W_1} \times 100 \quad (1)$$

2.5. Mechanical characterization of the fabricated microcapsules

The mechanical properties of the PMF shell microcapsules were conducted using the single-capsule compression test by Keller and Sottos [32]. Based on the good dispersibility of the fabricated microcapsules, single microcapsule was easily put at the end of the rod by carefully removing the surrounding extra microcapsules. Images of the

single microcapsule were taken prior to the compression test for the diameter measurement of the microcapsules tested. The loading rate for the stepper actuator (Physik Insurmente M-230S) was 2 μm/s and controlled via a computer interface. The load was acquired by a 0.5 N load cell (FUTEK).

2.6. Antibacterial test of the microcapsules

The antibacterial test was conducted based on the ASTM E2315 time-kill test standard to examine the antibacterial performance of the fabricated microcapsules against *V. coralliilyticus*, *E. coli and E. aestuarii*. Overnight culture of all the bacterial strains was prepared at 30 °C in marine broth 2216. The bacterial suspension was diluted in PBS to a concentration of approximately 1×10^6 cfu/ml for all three bacterial strains. Meanwhile, 0.2 g of the fabricated microcapsules were suspended in a dialysis bag. Subsequently, the dialysis bag containing microcapsules was brought into contact with the bacteria by immersing in 20 ml of the prepared PBS solution with an initial concentration of approximately 1×10^6 cfu/ml. At different time interval, 50 μL of bacterial suspension was removed and appropriate dilutions were carried out using PBS solution. The diluted bacterial suspensions were then aseptically spread on the marine agar 2216 plates. Lastly, the marine agar plates were incubated overnight at 30 °C and the number of surviving bacteria was determined through quantification of the number of colony forming unit (CFU). Based on the results of standard plate count method, the antibacterial activities of the microcapsules containing clove oil can be determined for each of the bacterial strains tested.

2.7. Characterization of multifunctional coating

2.7.1. Preparation of the coating

Multifunctional coating with anticorrosion and antibacterial properties was prepared based on the addition of multifunctional microcapsules containing 8-HQ and clove oil, serving as corrosion inhibitors and antimicrobial agent respectively. Mild steel plates ($50 \times 50 \times 2\ mm^3$) were used as the substrate for the multifunctional coatings. The steel plates were first polished using sand paper and washed with acetone and water to remove the impurities on the surface. The multifunctional coating was prepared by dispersing 20 wt% of the fabricated microcapsules in epoxy resin (Epolam 5015 and hardener 5014) and degassed in the vacuum for 15 min. Subsequently, the degassed epoxy resin containing 20 wt% of microcapsules was coated through brush method on the mild steel plate with a final thickness of around 350–400 μm. The prepared multifunctional resin was then cured for 2.5 h at 40 °C followed by spreading approximately 20 mg of fabricated microcapsules on the surface of the coating, resulting in multifunctional coatings with both fully and half embedded microcapsules. Lastly, the multifunctional coating was cured for another 12 h at room temperature before testing on its anticorrosion and antibacterial performance. The final thickness of the coatings was measured and verified using a coating thickness gage (PosiTector 6000).

2.7.2. Anticorrosion test

Multifunctional coating with embedded microcapsules was manually scratched using a razor blade and the uncoated areas of the steel plates were tightly covered using waterproof adhesive tape. Subsequently, the coating is immersed in 3.5 wt% NaCl solution for 24 h. The scratched areas were visually inspected to examine the anticorrosion performance based on the formation of rust. Additionally, to observe the underlying substrate, acetone was used to remove the coating under sonication. The underlying substrate was then characterized using SEM to examine the corroded areas if any and the formation of inhibition layer, which is responsible for the anticorrosion behavior of this multifunctional coating.

EIS measurement was performed on a Gamry Reference 600 Potentiostat via a conventional three-electrode system after different immersion duration in 3.5 wt% NaCl solution. Mild steels with blank epoxy coating and the fabricated multifunctional coatings were the working electrode The frequency range used was from 10^{-2} to 10^5 Hz with 10 steps per decade and the AC amplitude used was 10 mV. Similarly, Tafel plot was performed using 3.5 wt% NaCl solution as the electrolyte. The voltammograms were measured between +1.5 and −1.5 V at a scanned rate of 1 mV/s.

In addition to the FTIR studies of the inhibition layer, X-ray photoelectron spectroscopy (XPS) was conducted to examine the presence and chemical state of the elements on the corrosion inhibition layer. The formation of inhibition layer was scrap off from the scratched region of the multifunctional coating containing the fabricated microcapsules. Subsequently, XPS analysis of the sample was performed by using a Kratos Axis Supra Spectrometer with an Al Kα excitation radiation (1486.6 eV). The scanned size of the sample is 300 × 700 μm with an emission current of 15 mA. The wide and spectrum scans were conducted at 1 eV and 0.1 eV step size respectively.

2.7.3. Antibacterial test

The antibacterial performance of the multifunctional coating was evaluated based on zone inhibition test. Seawater bacteria isolated from Sebarok Island, Singapore was tested against the fabricated multifunctional coating to indicate the potential use of these coatings for treating marine fouling.

Seawater bacteria were grown in the marine broth 2216 at 30 °C overnight. Subsequently, 100 μL of the cloudy bacteria suspension was aseptically spread onto the marine agar 2216 plates using a sterile swab. To conduct the zone inhibition test, the multifunctional coatings were then placed at the center of the agar plates, with the effective antibacterial surface in contact with the marine agar surface. The marine agar plates were then incubated at 30 °C for 24 h and the antibacterial performance of the coatings was evaluated based on the presence of inhibition zone around the coatings.

3. Results and discussion

3.1. Formation mechanism of PMF shell

The formation mechanism of poly (melamine-formaldehyde) PMF shell can be divided into two different stages – nucleophilic addition reaction and acid condensation stage. During the first stage, the prepolymer solution of melamine-formaldehyde was prepared at 70 °C for 1 h. The nucleophilic addition reaction of melamine to formaldehyde leads to the formation of methylolmelamine under basic conditions. Subsequently, under acid condensation stage, a large number of oligomer derivatives and crosslinked network are formed and eventually deposit on the surface of the emulsified core material droplets as the molecular weight increases. Finally, crosslinking occurs to form a dense PMF shell encapsulating the core materials – 8-HQ and clove oil [33]. Additionally, the addition of PVA serves to protect the colloids and prevent the newly formed capsules from sticking to each other, which eventually increase the yield of the microencapsulation process [31].

3.2. Morphology of microcapsules and shell structure

Scanning electron microscopy (SEM) was used to characterize the structure of the microcapsules, in term of the shape, size, shell thickness and surface morphology of the fabricated microcapsules. According to Fig. 1(a), the resultant microcapsules are spherical in shape with a diameter of 98 ± 15 μm while the size distribution of the fabricated microcapsules is shown in Fig. 1(d). The rough surface morphology of the microcapsules as shown in Fig. 1(b) is formed through the deposition of melamine-formaldehyde nanoparticles on the stable core material droplet as the PMF molecular weight increases. Additionally, the cross-sectional view of the microcapsules is shown in Fig. 1(c), showing a dense PMF shell with thickness of 3.7 ± 0.7 μm, which renders them

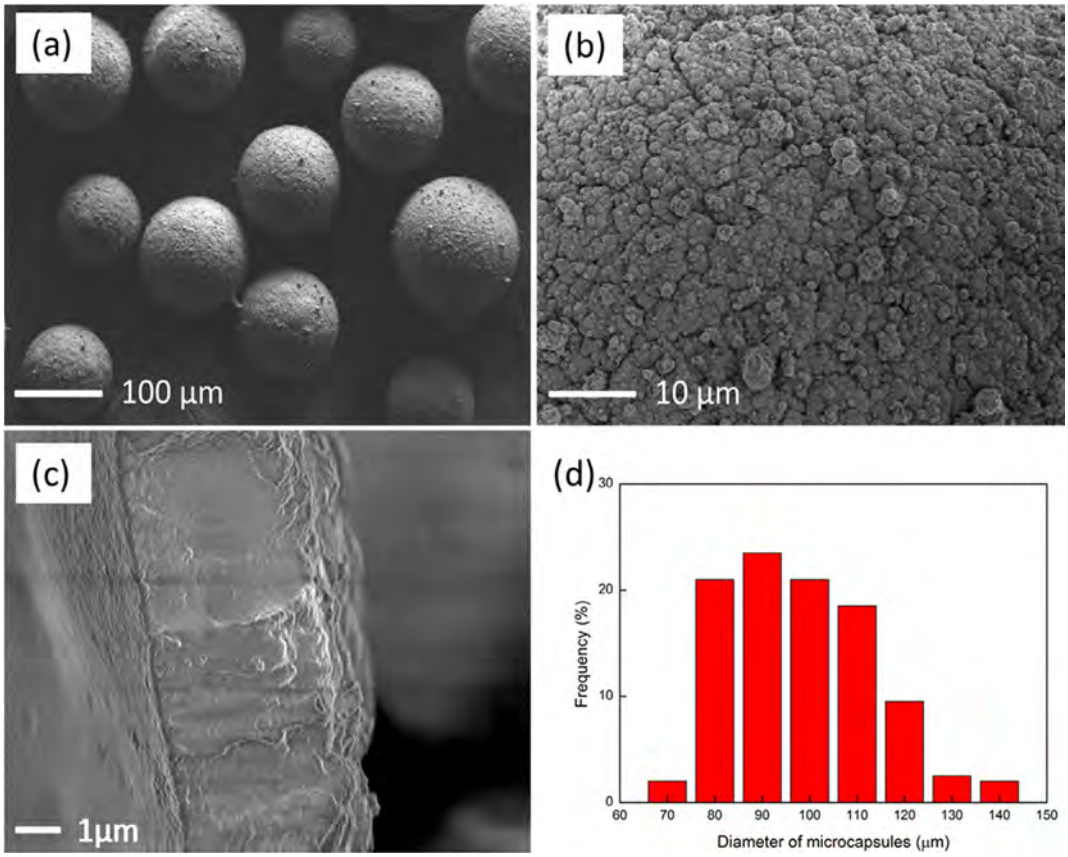

Fig. 1. FESEM characterization of the fabricated microcapsules showing (a) spherical shape without any agglomeration problem; (b) rough surface morphology; (c) dense PMF shell with shell thickness of 3.7 ± 0.7 µm; (d) microcapsules size distribution, giving an average size of 98 ± 15 µm.

with excellent mechanical strength.

3.3. Determination of microcapsules content

Fig. 2 shows the FTIR spectra of clove oil, 8-HQ, mixture of clove oil and 8HQ and core material. The spectrum of the core material is similar to that of the mixture of clove oil and 8-HQ, proving successful encapsulation of the mixture. The addition of 8-HQ compound into clove oil is confirmed through the peak near 1580 cm^{-1}, which corresponds to C═N stretching. Additionally, the peak at 1400 cm^{-1} and 1090 cm^{-1} represents C—N stretching. These peaks confirm the presence of nitrogen in the mixture, which is essential for the corrosion inhibition properties of the 8-HQ compound.

3.4. Core fraction

The core contents of the fabricated microcapsules after different storage time in the glass vial were measured using the solvent extraction method. According to Fig. 3, the initial core content of the fabricated microcapsules is 81.0 ± 0.8%. As the storage time in the glass vial prolongs, the core content of the microcapsules decreases to

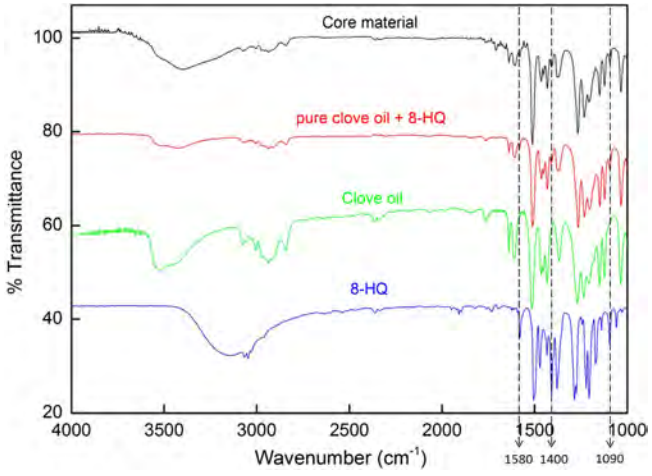

Fig. 2. FTIR spectra of 8-HQ, mixture of clove oil and 8-HQ, clove oil and the encapsulated core material.

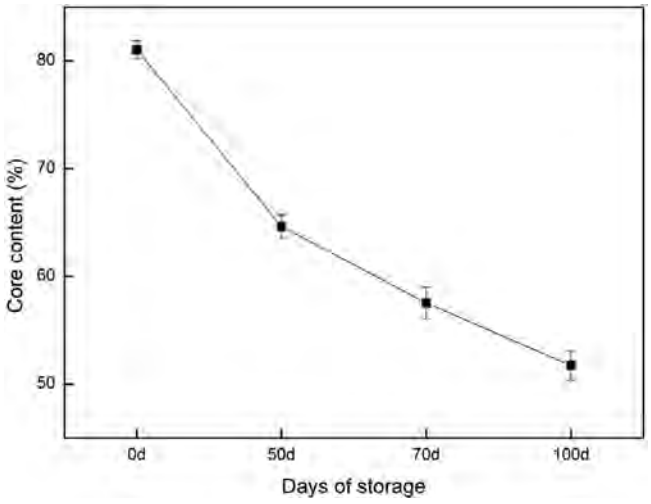

Fig. 3. Effect of storage period on the core content of the fabricated microcapsules.

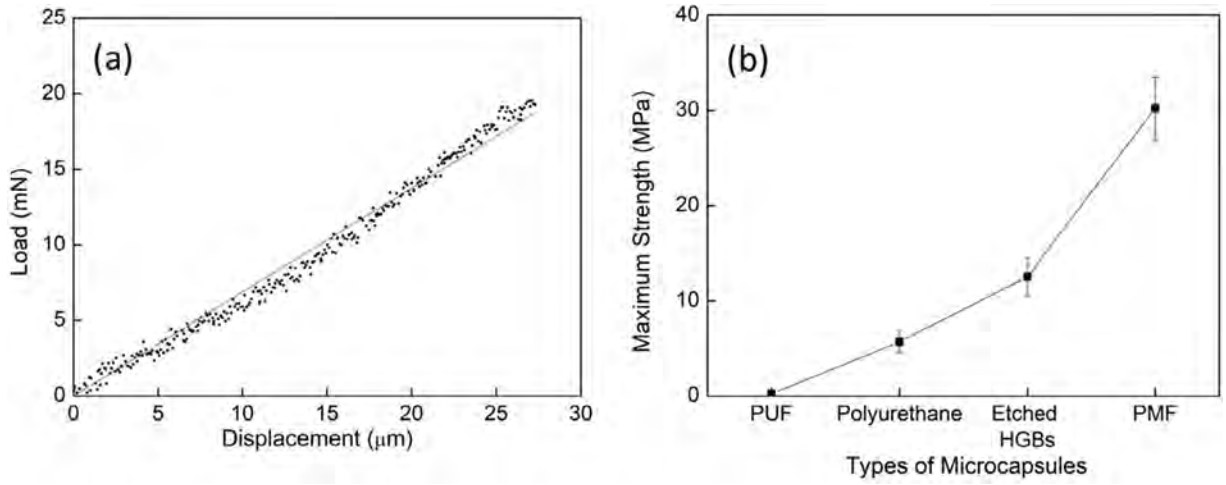

Fig. 4. (a) Load-displacement curve of the fabricated PMF shell microcapsules; (b) Comparison of normalized maximum strength between microcapsules with different shells and the fabricated PMF shell microcapsules.

64.6 ± 1.1%, 57.5 ± 1.5% and 51.7 ± 1.4% after storage period of 50, 70 and 100 days respectively. The dense PMF shell of the microcapsules preserves the core material from premature leakage and the percentage decrease of the core content was maintained to be less than 40% even after 100 days of storage in the glass vial.

3.5. Compressive property

The mechanical strength of the fabricated microcapsules was investigated using the single-capsule compression test [32]. The diameter of the tested microcapsules was measured based on the known diameter of the compression rod, which is 2 mm. Fig. 4(a) shows the load-displacement curve of the PMF shell microcapsules under compression and the maximum load of the tested microcapsules was 18.8 ± 0.9 mN. Additionally, the PMF shell microcapsules display brittle failure mode, which is clearly observed from the load-displacement curve. The normalized maximum strength, σ_{max} of the microcapsules can be calculated using the formula below [34]:

$$\sigma_{max} = \frac{4P_{max}}{\pi(D_o^2 - D_i^2)} \quad [2]$$

where P_{max} is the maximum load, D_o and D_i are the outer and inner diameter of the PMF shell microcapsules respectively. Based on this formula, the calculated maximum strength of the fabricated PMF shell microcapsules is 30.2 ± 3.3 MPa and is compared with the maximum strength of the urea-formaldehyde shell [32], polyurethane shell microcapsules [34] and etched hollowed glass bubbles (HGBs) [35], which were all measured using the similar single-capsule compression test setup. According to the summary in Fig. 4(b), the strength of fabricated PMF shell microcapsules is an order of magnitude and 5 times higher than the strength of PUF and polyurethane shell microcapsules respectively. Additionally, the strength is also more than twice the strength of hollow glass bubbles (HGBs), which was previously shown to possess high strength as a non-polymer reservoir. These comparisons demonstrate the robustness of the fabricated PMF shell microcapsules, which could potentially improve the practical use of these microcapsules in a wider range of applications.

3.6. Antibacterial performance

Vibrio is a genus that contains a wide range of marine bacteria species, which were usually used to examine the effectiveness of different antifouling coatings and surfaces [36]. Among the *Vibrio* bacteria species, *Vibrio coralliilyticus* is a globally distributed bacterium with temperature dependent pathogenicity in the coral and also one of the bacteria found in the marine biofilm [37]. Additionally, *Escherichia coli* are another type of bacteria that was previously found on the ship hull, which is one key area of biofouling that has caused huge economic losses due to the increasing fuel consumption. *Exiguobacterium* is another bacteria species found in the marine environment and *E. aestuarii* is another marine bacterium used in this study to examine the antibacterial effect of the fabricated microcapsules against a wider range of marine bacteria species. The development process of biofouling is usually initiated by the adhesion of marine bacteria to form biofilm, which serves as the nutrient sources of the subsequent attachment of fouling organisms. Hence, *V. coralliilyticus, E. coli* and *E. aestuarii* were used as the sample marine bacteria in the antibacterial test to indicate the potential use of the fabricated microcapsules in tackling biofouling problem.

The antibacterial activity of the fabricated microcapsules against *E. coli*, *V. coralliilyticus* and *E. aestuarii* was systematically investigated using the ASTM E2315 time-kill test. Figs. 5–7 show the antibacterial effect of the fabricated microcapsules against *E. coli, V. coralliilyticus* and *E. aestuarii* respectively. As compared to the control sample, the addition of fabricated microcapsules resulted in decreasing number of colony counts for all three bacteria tested at increasing contact time. As the number of colony counts represents the amount of surviving bacteria, the antibacterial effect of the microcapsules against three different marine bacteria tested is clearly demonstrated through this time-kill test.

According to Fig. 5, as the contact time prolongs, the number of surviving *E. coli* decreases and they were completely killed at 48 h of contact time. Similar effect was observed against *V. coralliilyticus* and *E. aestuarii* as shown in Figs. 6 and 7 respectively, in which the released core materials from the fabricated microcapsules successfully kill the bacteria completely after 24 h of contact time. The antibacterial behavior of the microcapsules originates from the interaction between the released clove oil and the bacteria cell membrane, which disrupts and permeabilizes the membrane to cause leakage of nutrients required for healthy cell growth [38–40]. Additionally, 8-HQ was proven to exhibit antimicrobial activity against a wide range of bacteria strains based on its ability to chelate metal ions that are essential for the metabolic processes [41]. Hence, it can be hypothesized that both clove oil and 8-HQ contributes to the antibacterial properties of the fabricated microcapsules.

Nevertheless, the antibacterial effect of the fabricated microcapsules containing 20 wt% 8-HQ dissolved in clove oil was compared against that of microcapsules containing only clove oil and 8-HQ respectively to further understand the antibacterial mechanism. Fig. 8 shows the bacterial viability of *E. coli* at different time interval for different types of

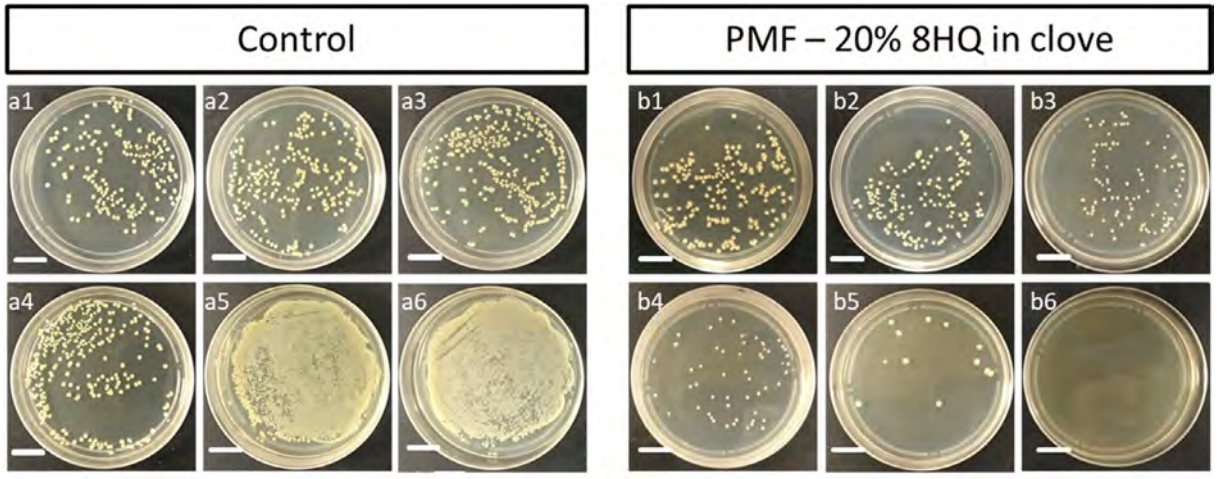

Fig. 5. Time-kill test against *E. coli* at different time intervals: (a1) 0 h; (a2) 4 h; (a3) 8 h; (a4) 11 h; (a5) 24 h; (a6) 48 h for control sample without any microcapsules; (b1) 0 h; (b2) 4 h; (b3) 8 h; (b4) 11 h; (b5) 24 h; (b6) 48 h for synthesized microcapsules. Scare bar represents 2 cm.

microcapsules. It is apparent that all three types of microcapsules with different core materials exhibit antibacterial behavior with similar trend. The antibacterial effect of PMF shell microcapsules containing only clove oil was observed earliest as compared to the other two as complete killing was observed after 24 h of contact with *E. coli*. Hence, it can be hypothesized that clove oil plays a more important role for the antibacterial effect of the fabricated microcapsules. Additionally, it is important to highlight that the presence of 8-HQ does not compromise the antibacterial effect of the released clove oil from the microcapsules. However, as the antibacterial effect of the fabricated microcapsules containing the mixture of 8-HQ and clove oil was not observed earlier as compared to that of the microcapsules containing clove oil, it can be concluded that there is no synergistic antibacterial effect based on the mixture of these two compounds. Nevertheless, clove oil was proven to be an effective antibacterial agent in the fabricated microcapsules, other than serving as an environmental friendly solvent for encapsulating 8-HQ.

3.7. Characterization of multifunctional coating

A multifunctional coating based on the addition of the microcapsules containing 8-HQ and clove oil was fabricated and the proposed antibacterial and anticorrosion mechanisms of the coating are demonstrated as shown in Fig. 9. To fabricate the multifunctional coatings, the microcapsules are partially embedded in the epoxy matrix, which can be achieved by spreading the microcapsules on the epoxy surface after curing for 2.5 h at 40 °C. As the epoxy matrix is partially cured, it becomes more viscous and prevents the microcapsules from completely sinking to the bottom. As a result, an epoxy coating with both fully and partially embedded microcapsules can be synthesized as the schematic diagram shown in Fig. 9(a). To confirm the feasibility of this method in producing partially embedded microcapsules in the epoxy matrix, SEM characterization on the multifunctional coating was conducted. On the basis of Fig. 10, the partially embedded microcapsules were clearly observed on the epoxy matrix, indicating the successful fabrication of this surface feature of approximately half-embedded microcapsules on epoxy coating through manipulating the curing process.

The time-kill antibacterial test from the previous section has demonstrated the antibacterial properties of the fabricated microcapsules against different types of bacteria. Similarly, the proposed antibacterial mechanism of the multifunctional coating is shown in Fig. 9(a), depicting the released clove oil from the microcapsules, which eventually disrupts the cell membrane and causes cell death [38–40]. Additionally, the multifunctional coating possesses anticorrosion properties through the fully embedded microcapsules. Any physical damage to the coating may expose the underlying substrate but at the same time releasing the core material from the ruptured microcapsules, which eventually forms a corrosion inhibition layer to retard corrosion attack. To confirm on

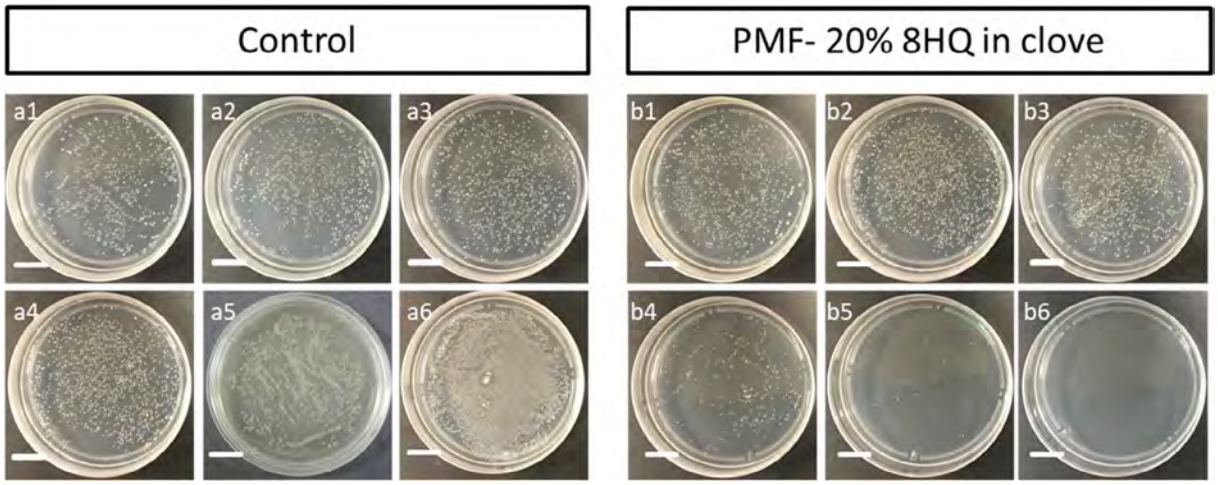

Fig. 6. Time-kill test against *V. coralliilyticus* at different time intervals: (a1) 0 h; (a2) 1 h; (a3) 3 h; (a4) 5 h; (a5) 7 h; (a6) 24 h for control sample without any microcapsules; (b1) 0 h; (b2) 1 h; (b3) 3 h; (b4) 5 h; (b5) 7 h; (b6) 24 h for synthesized microcapsules. Scare bar represents 2 cm.

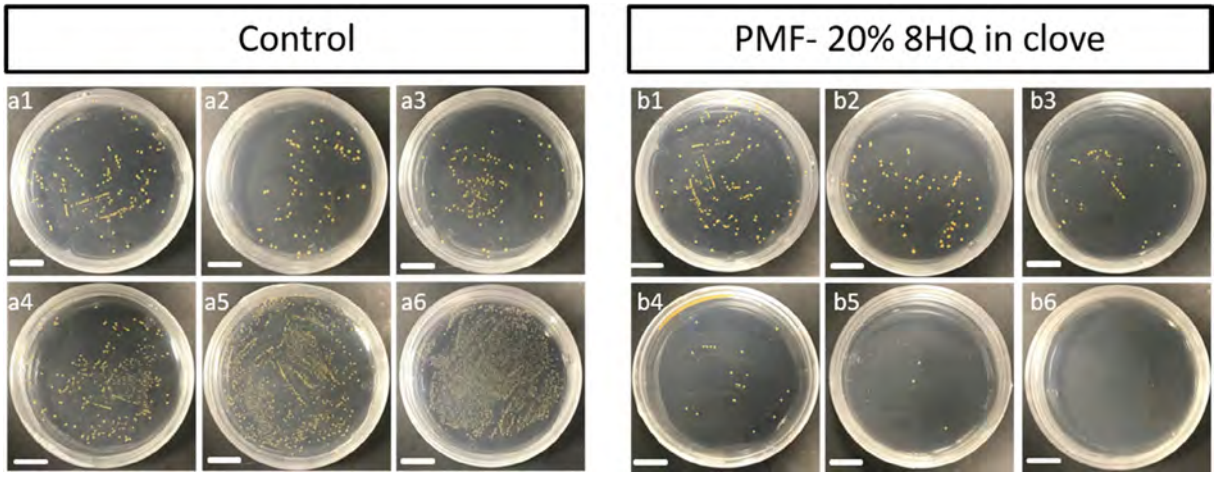

Fig. 7. Time-kill test against *E. aestuarii* at different time intervals: (a1) 0 h; (a2) 3 h; (a3) 5 h; (a4) 7 h; (a5) 9 h; (a6) 24 h for control sample without any microcapsules; (b1) 0 h; (b2) 3 h; (b3) 5 h; (b4) 7 h; (b5) 9 h; (b6) 24 h for synthesized microcapsules. Scare bar represents 2 cm.

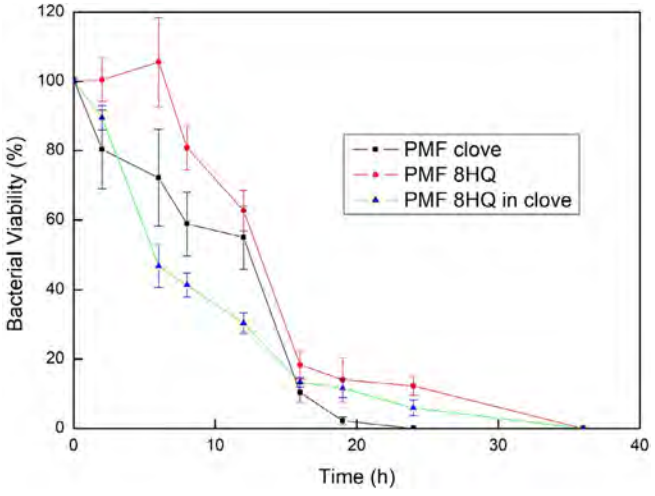

Fig. 8. Comparison of antibacterial effect of microcapsules containing different core material: clove oil, 8-HQ dissolved in toluene and 8-HQ dissolved in clove oil.

the hypothesized multifunctional mechanisms, antibacterial and anticorrosion tests were conducted systematically and discussed as followed.

3.7.1. *Antibacterial behavior of the coatings*

As discussed earlier, the time-kill test results have indicated the excellent antibacterial performance of the microcapsules against *E. coli* and *V. coralliilyticus*. Subsequently, the fabricated microcapsules were deposited onto the multifunctional coatings as shown in Fig. 10. Zone inhibition test was conducted on the fabricated multifunctional coating to determine its antibacterial properties against the seawater bacteria. Together with the respective antibacterial test against different marine bacteria strain for the fabrication microcapsules, this zone inhibition test against the seawater bacteria serves as a comprehensive indication on the potential antifouling performance of the fabricated multifunctional coatings for the marine industry.

According to Fig. 11, a clear inhibition area was observed around the multifunctional coating while the bacteria are viable around the blank epoxy coating without any inhibition area formed. Thus, it can be concluded that the epoxy coating containing the multifunctional microcapsules possess excellent antibacterial performance against the seawater bacteria due to the addition of the fabricated microcapsules. The antibacterial performance of the coatings originates from the released core materials from the microcapsules submerged on the surface

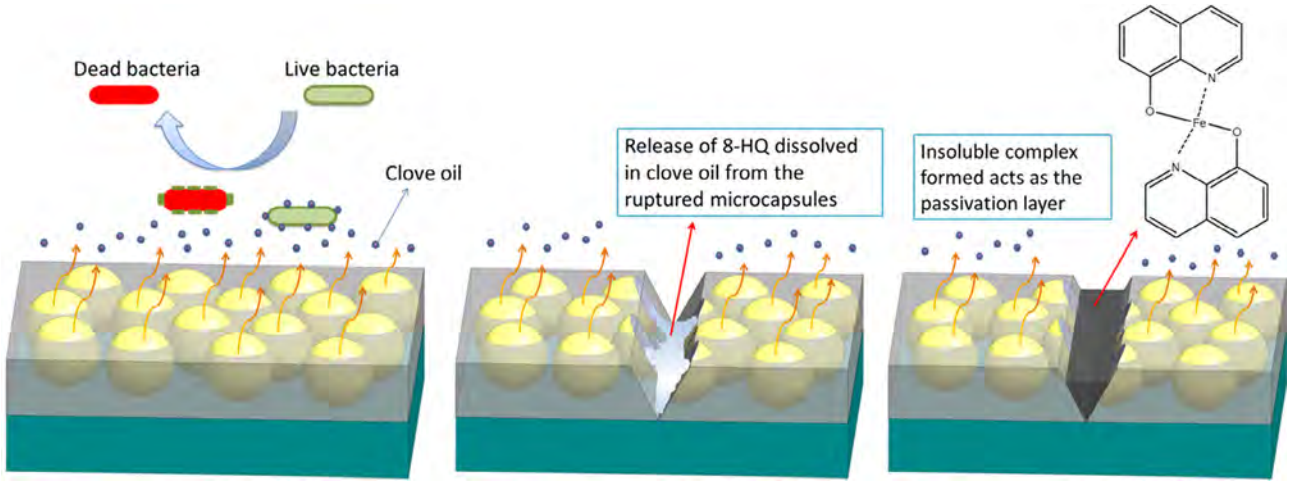

Fig. 9. Mechanism of multifunctional coatings with antibacterial and anticorrosion features: (a) antibacterial effect of the coating based on the released clove oil from the microcapsules; (b) upon mechanical damage to the coating, the 8-HQ dissolved in clove oil is released from the broken microcapsules; (c) the reaction of 8-HQ with the exposed steel substrate forms an insoluble complex to act as a passivation layer to retard corrosion attack.

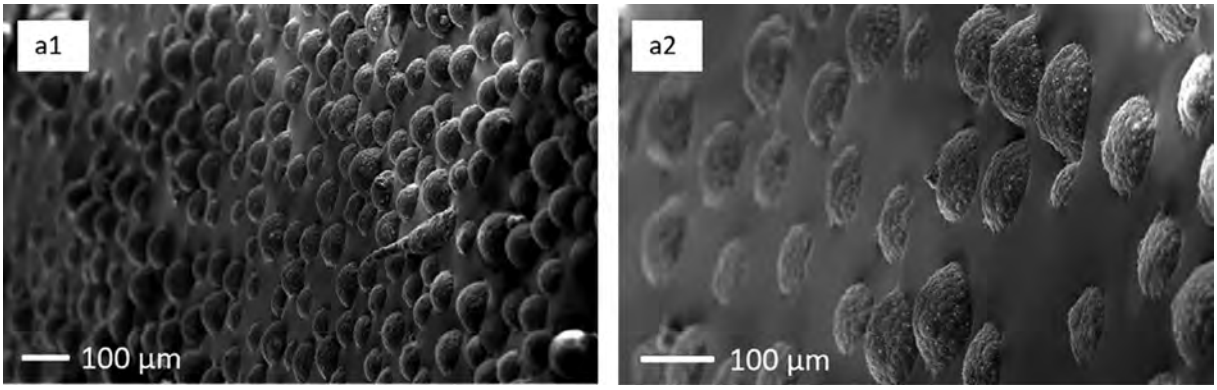

Fig. 10. Fabrication of epoxy with partially embedded microcapsules through controlling the curing time of the epoxy matrix.

of the coating, which diffuse across the marine agar and inhibit the growth of the seawater bacteria around the coating, indicating the potential of this multifunctional coating for marine antifouling applications. In conclusion, the excellent antibacterial performance through zone inhibition test further confirms the antibacterial mechanism proposed in the schematic diagram shown in Fig. 9(a), which is related to the released core materials from the surface in achieving excellent antibacterial performance.

3.7.2. Anticorrosion performance

Corrosion remains as an unsolved problem to date in the marine industry. Physical damage to the coating may occur and result in the exposure of underlying substrate to the corrosive marine environment. As discussed earlier, the fabricated microcapsules possess excellent antibacterial performances as proven from the time-kill test results while the antibacterial performance of the multifunctional coatings containing the fabricated microcapsules was verified through the zone inhibition test. Additionally, the anticorrosion features of the multifunctional coating containing fabricated microcapsules in protecting the underlying substrate from corrosion attack were studied.

To evaluate the anticorrosion performance, pure epoxy coating as a control, epoxy coating with 8-HQ compound directly added through dissolving in xylene and multifunctional epoxy coating with embedded microcapsules were manually scratched using a razor blade and subsequently immersed in a 3.5 wt% NaCl aqueous solution at room temperature for 24 h. A physical scratch was made on the coating to simulate the physical damage that may occur during the industrial uses in the marine industry. According to Fig. 12, severe rust was formed and observed on the pure epoxy coating and epoxy coating with 8-HQ compound directly added while the scratched areas of the multifunctional coating with embedded microcapsules were completely free of rust. Superior anticorrosion performance of the coating originates from the addition of the fabricated microcapsules containing 8-HQ compound, which possess excellent corrosion inhibition properties. According to Fig. 12(c), it is apparent that some black color solids were formed at the scratched region, which prevents the formation of rust as observed in both Fig. 12(a) and (b) for epoxy coating with 8-HQ directly added through dissolving in xylene and blank epoxy coating respectively.

The anticorrosion mechanism of the multifunctional coating is illustrated according to the schematic diagram shown in Fig. 9(b) and (c). Fig. 9(b) demonstrates the release of 8-HQ dissolved in clove oil from the broken microcapsules upon mechanical damage to the coating. Immediately after the breakage of microcapsules, the released 8-HQ compounds react with the iron atom from the steel substrate to form a corrosion inhibition layer that acts as a barrier between steel surface and corrosive medium. As shown in Fig. 9(c), the protective barrier formed can retard corrosion attack through preventing or minimizing the dissolution of corrosion species such as Cl^- ions and O_2 gas. Based on the visual inspection of the coating immersed in a 3.5 wt% NaCl solution, black color substances were formed in the scratched region shortly after the mechanical damage occurs, showing the immediate response of the coating to inhibit further corrosion damage. The anticorrosion process was further characterized using Electrochemical Impedance Spectroscopy (EIS). According to Fig. 12(d), the impedance modulus (Z_{mod}) of the epoxy coating containing multifunctional

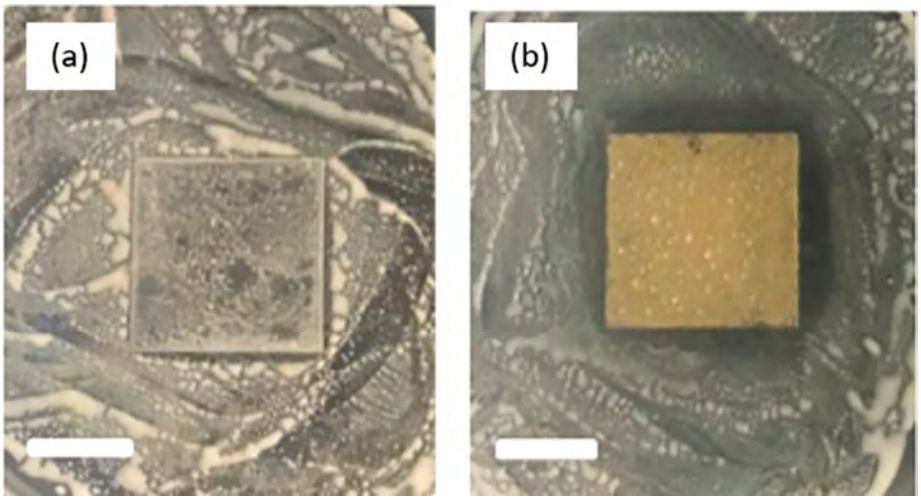

Fig. 11. Zone inhibition test against seawater bacteria for (a) blank epoxy coating showing no inhibition area and (b) epoxy coating containing fabricated multifunctional microcapsules showing an inhibition area around the coating. Scale bar is 1 cm.

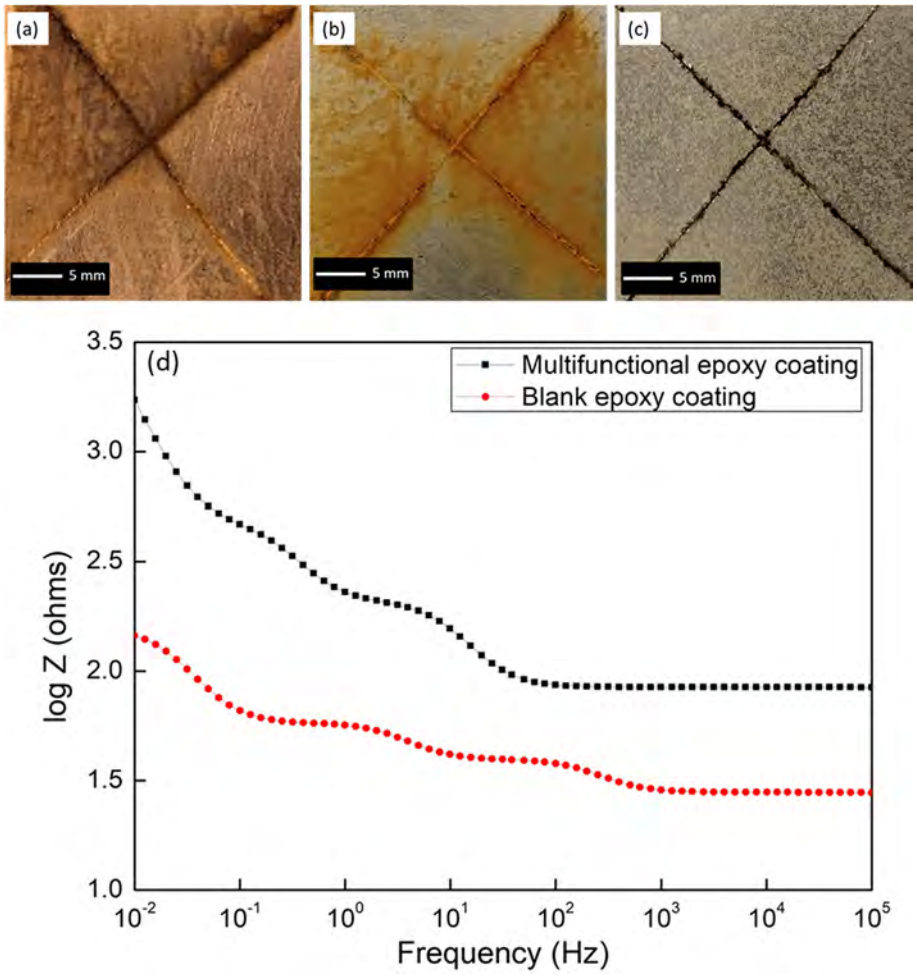

Fig. 12. Optical images after one-day immersion in 3.5 wt% NaCl solution for (a) epoxy coating with 8-HQ directly added during the epoxy curing process, (b) epoxy coating and (c) epoxy coating with 20 wt% of PMF shell multifunctional microcapsules. (d) The electrochemical impedance of the scratched epoxy coatings containing multifunctional microcapsules after 1 day immersion in 3.5 wt% NaCl solution.

microcapsules is different as compared to the blank epoxy coating. In particular, the impedance at low frequencies can be related to the processes occurred at the scratched defect region. The impedance modulus value of the microcapsules-based multifunctional epoxy coating is higher as compared to the blank epoxy coating, owing to the formation of inhibition layer formed at the scratched region. According to previous research, the adsorption of these molecules is through chemisorption, which involves the charge sharing or transfer from the nitrogen molecules to the iron atom from the metal surface to form a coordinate type bond [42].

Additionally, it is important to highlight that the formation of rust at the scratched region of the epoxy coating with 8-HQ directly added indicates the loss of corrosion inhibition properties from the 8-HQ compounds. Without encapsulation, the undesirable interaction between 8-HQ and the epoxy matrix during the curing process may result in the premature loss of corrosion inhibition properties, causing the formation of rust at the scratched region. On the contrary, by encapsulating 8-HQ compound through in-situ polymerization process, the corrosion inhibition properties were preserved to successfully prevent corrosion attack upon physical damage to the coating, such as the formation of scratches.

To further investigate the anticorrosion performance of the coatings, SEM characterizations were conducted on the underlying steel substrate of both blank epoxy coating and multifunctional coating with 20 wt% of microcapsules containing 8-HQ compound dissolved in clove oil after immersed in 3.5 wt% NaCl solution for 10 days. According to Fig. 13, the improved anticorrosion performance based on the addition of multifunctional microcapsules containing clove oil and 8-HQ was observed. According to Fig. 13(a), large corroded areas were observed around the scratched region, which were resulted from the penetration of corrosive medium across the scratch, causing more material losses around the scratches. This indicates the poor sealing effect of the blank epoxy coating which allows the penetration of corrosive medium across the scratches made.

On the contrary, these corroded areas were not observed around the scratched regions of the multifunctional coatings containing fabricated microcapsules as proven by the optical images shown in Fig. 13(b). Because of the presence of the corrosion inhibition layer, the penetration of corrosive medium is inhibited and hence, the corrosion attack was retarded both at the scratched region and the areas around the scratched regions. Additionally, Fig. 13(c) shows the formation of black color corrosion inhibition layer on the steel surface outside of the scratched regions. The formation of these black dots is related to the slow diffusion of 8-HQ compound from the microcapsules over time to react with the steel surface. Nevertheless, the diffusion of 8-HQ compound is relatively slow and does not compromise the in-situ corrosion inhibition effect of the coatings as shown and discussed in the next section (Fig. 14).

Additionally, the barrier properties of the unscratched coatings were characterized using Tafel plots. The Tafel plots of the blank epoxy coatings and multifunctional epoxy coatings after 10 days of immersion in 3.5 wt% NaCl solution were shown in Fig. 13(d). The electrochemical

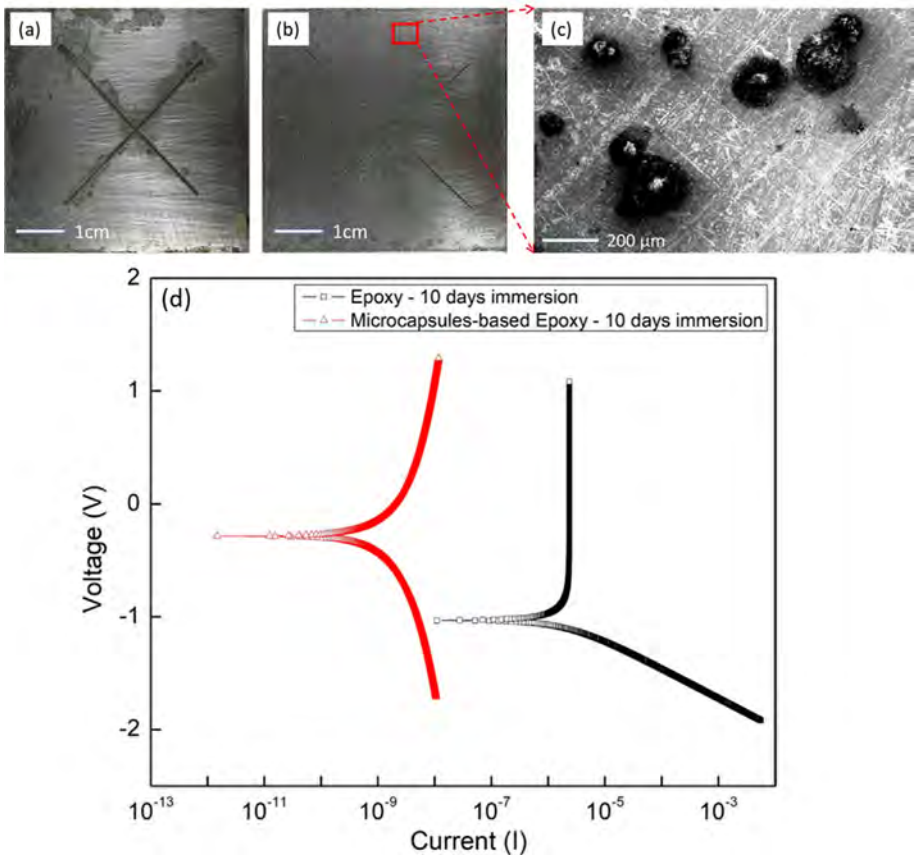

Fig. 13. Optical images of underlying steel substrate for (a) blank epoxy coating and (b) multifunctional coating containing fabricated microcapsules, in which the SEM images indicates (c) the formation of dark color corrosion inhibition layer as a result of the reaction between the released 8-HQ compound and steel surface. (d) Tafel plot for unscratched blank epoxy coatings and microcapsules-based epoxy coatings after 10 days of immersion in 3.5 wt% NaCl solution.

corrosion parameters including the corrosion potential (E_{corr}) and corrosion current (I_{corr}) are summarized and tabulated in Table 1. The I_{corr} of the coatings is related to the diffusion of electrolyte across the coating, which will eventually cause corrosion on the underlying metal substrate. Hence, a lower I_{corr} represents lower coating degradation over time and the better barrier properties of coatings. By comparing the electrochemical corrosion measurement results, it is apparent that the addition of microcapsules decreases the current density of the coatings. The I_{corr} of the multifunctional microcapsules-based coatings was lower than that of the blank epoxy coatings after 10 days of immersion in 3.5 wt% NaCl solution, indicating that the barrier properties of the microcapsules-based coatings were better to prevent the diffusion

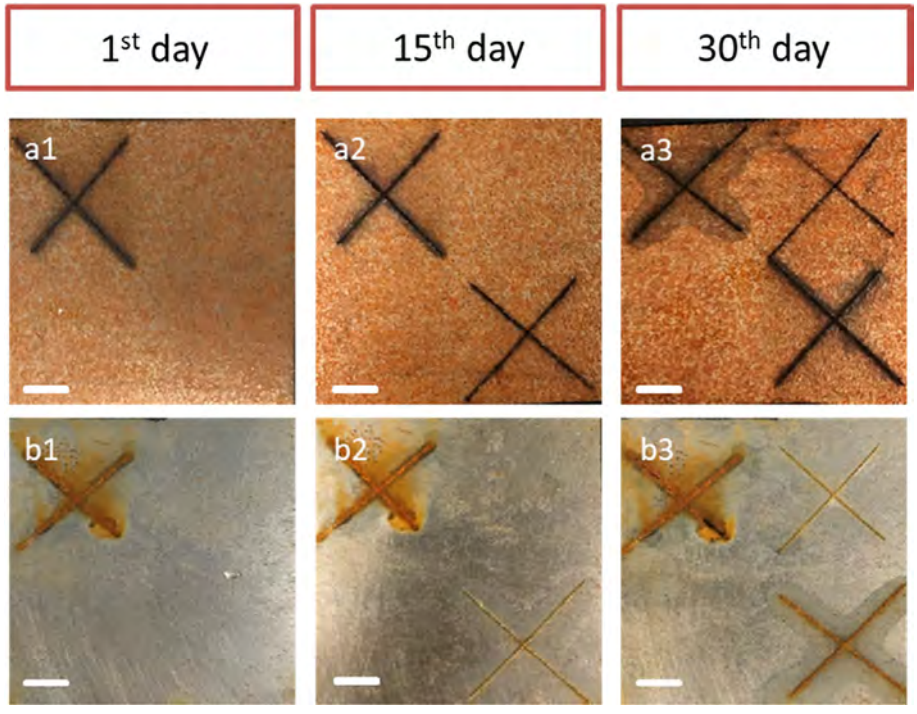

Fig. 14. Long-term stability of the fabricated microcapsules in anticorrosion coating allows the effective formation of dark color complexes after multiple scratches made on the: (a1) 1st day, (a2) 15th day and (a3) 30th day of immersion in 3.5% NaCl solution. Rust formation was clearly observed in epoxy coating after multiple scratches made on the: (b1) 1st day, (b2) 15th day and (b3) 30th day of immersion in 3.5% NaCl solution.

Table 1
Electrochemical corrosion measurements from Tafel plots for blank epoxy coatings and microcapsules-based epoxy coatings after 10 days of immersion in 3.5 wt% NaCl solution.

	Immersion period (days)	E_{corr} (mV)	I_{corr} (nA)
Blank epoxy coating	10	−1030	2380
Microcapsules-based epoxy coatings	10	−284	8.020

of corrosive medium and ions across the coatings. As observed from Fig. 13(a), some delamination occurs for the blank epoxy coatings as corrosion marks were observed on the underlying substrate. However, this was not observed on the substrate with multifunctional epoxy coatings as shown in Fig. 13(b). Hence, with the supplement of the quantitative analysis from Tafel plot, it can be concluded that the microcapsules-based multifunctional epoxy coatings possess better barrier properties as compared to the blank epoxy coatings, indicating good adhesion between the microcapsules and epoxy coating matrix due to the rough surface morphology of the microcapsules.

Overall, by comparing the anticorrosion performance of different coatings, it can be concluded that the encapsulation of 8-HQ is essential to simultaneously prevent the undesirable interaction of 8-HQ with the epoxy matrix and allow in-situ corrosion inhibition to occur upon the release of 8-HQ from the broken microcapsules during the event of physical damage on the coatings.

3.7.3. Microcapsules long term stability

Long term stability of the microcapsules-based multifunctional epoxy coatings for anticorrosion protection was examined by scratching the coating after immersion in 3.5 wt% NaCl solution for an extended period of time up to 30 days. Fig. 14 illustrates the long-term anticorrosion effectiveness of the microcapsules-based epoxy coatings as the black color inhibition layers are formed upon scratching even after 30 days of immersion in 3.5% NaCl solution, retarding the corrosion attack and protecting the underlying substrate. Additionally, the corrosion inhibition layer remains at the scratched region after 30 days of immersion without being washed off into the solution. On the contrary, dense rust was formed at the scratched regions of blank epoxy coating, indicating no corrosion protection. Hence, it can be concluded that the fabricated multifunctional microcapsules possess excellent stability in the salt water, allowing in-situ sealing of any scratch damages with the formation of corrosion inhibition layer for an extended period of time.

3.7.4. Chemical structure of corrosion inhibition layer

The chemical structure of the newly formed corrosion inhibition layer was examined using FTIR spectroscopy. The black color solid formed at the scratched region were scrapped and collected for FTIR characterization. Based on the characterization results as shown in Fig. 15, there are several shifts in the absorption peaks for the corrosion inhibition layer formed as compared to the original 8-HQ compound. Based on the comparison, the peak occurred at 1093 cm^{-1} for 8-HQ, which corresponds to the C—O vibrations, is shifted to 1107 cm^{-1} for the insoluble complex. Additionally, the shift in the absorption peak, from 3142 to 3427 cm^{-1} indicates the change of OH bond in the newly formed corrosion inhibition compound. As a result, the shift of these peaks indicates the interaction of oxygen atom with the metal surface atoms. Moreover, the absorption peaks at 1506 and 1579 cm^{-1} are due to C=N stretching in the original 8-HQ compound. These peaks are slightly shifted to 1494 and 1575 cm^{-1} respectively, indicating the change of vibration frequencies of this bond resulted from the interaction of nitrogen atom with the metal surface atoms.

Additionally, the chemical structure of the corrosion inhibition layer was further confirmed through XPS analysis. According to Fig. 16(a), a high energy peak was observed at the binding energy of 709 eV, which corresponds to the presence of iron in FeO chemical state. Hence, this can be related to the presence of the bonding between the iron atom and oxygen from the 8-HQ compound. Moreover, Fig. 16(b) indicates a higher energy peak at the binding energy around 397 eV in the XPS spectrum of the corrosion inhibition layer. This high energy peak corresponds to the presence of nitrogen in metal nitrides chemical state, which can be related to the presence of bonding between nitrogen from the 8-HQ compound and the iron atom from the steel substrate. Based on the presence of iron and nitrogen atoms through XPS analysis, the chemical structure of the corrosion inhibition layer is predicted to that shown in Fig. 17 [11,43,44].

4. Conclusion

In summary, PMF shell microcapsules containing 8-HQ and clove oil, featuring good mechanical properties, anticorrosion, and antibacterial properties, were synthesized using in-situ polymerization methods. The fabricated microcapsules possess good mechanical properties, with higher strength as compared to the strength of PUF and polyurethane shell microcapsules, and the strength of hollow glass bubbles (HGBs). Time-kill test results determine the excellent antibacterial performance of the microcapsules against *V. coralliilyticus*, *E. coli and E. aestuarii*, as the representative marine bacteria in this study. Additionally, zone inhibition test reveals the antibacterial behavior of multifunctional coating containing the fabricated microcapsules against the seawater bacteria isolated from Sebarok Island, Singapore, indicating the potential of the coatings for marine antifouling applications. The anticorrosion properties were examined by immersing the

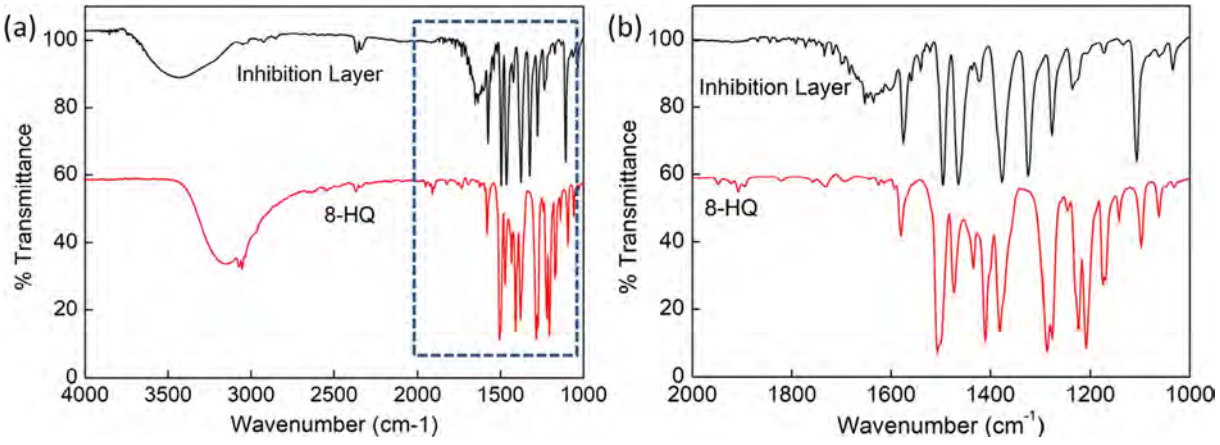

Fig. 15. (a) Comparison of FTIR spectra of insoluble complex and 8-HQ compound; (b) Zoomed-in spectra in the range of 1000–2000 cm^{-1}.

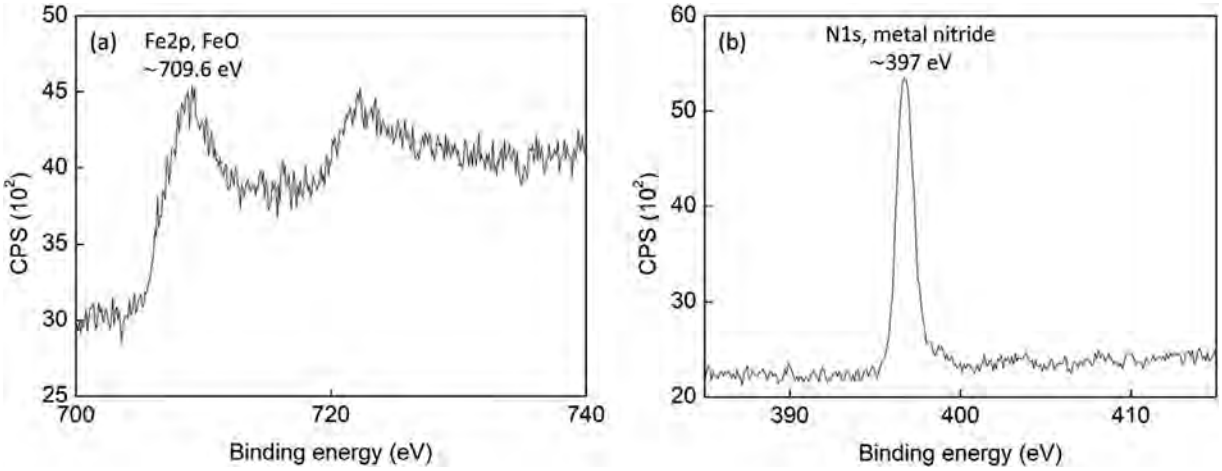

Fig. 16. XPS analysis of the insoluble complexes showing the presence of (a) iron atom in the chemical state of FeO with binding energy of 790.6 eV and (b) nitrogen atom in the chemical state of metal nitride with binding energy of 397 eV.

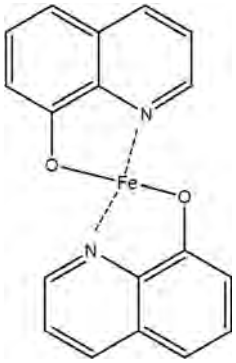

Fig. 17. Predicted chemical structures for the insoluble complexes based on literature [11,43,44], supported by FTIR and XPS analysis respectively.

scratched multifunctional coatings in 3.5 wt% NaCl solution. The physical damage on the coatings releases the 8-HQ compound from the broken microcapsules, which react with the iron atoms from the steel surface to form a corrosion inhibition layer. According to the SEM characterization results, the formation of corrosion inhibition layer successfully retards corrosion attack at and around the scratched regions, by preventing the diffusion of corrosive medium across the scratches. FTIR and XPS analysis were employed to examine and predict the chemical structure of the corrosion inhibition layer, which agrees well with the proposed structure from the previous studies.

Notes

The authors declared no competing financial interests.

Acknowledgement

We are grateful to the support partially from the Hong Kong University of Science and Technology (Grant #: R9365). Chong acknowledges the research scholarship support from NTU.

References

[1] M. Finšgar, J. Jackson, Application of corrosion inhibitors for steels in acidic media for the oil and gas industry: a review, Corros. Sci. 86 (2014) 17–41.
[2] F. Bentiss, M. Traisnel, M. Lagrenee, The substituted 1, 3, 4-oxadiazoles: a new class of corrosion inhibitors of mild steel in acidic media, Corros. Sci. 42 (1) (2000) 127–146.
[3] J. Aljourani, K. Raeissi, M. Golozar, Benzimidazole and its derivatives as corrosion inhibitors for mild steel in 1M HCl solution, Corros. Sci. 51 (8) (2009) 1836–1843.
[4] G. Gece, Drugs: a review of promising novel corrosion inhibitors, Corros. Sci. 53 (12) (2011) 3873–3898.
[5] G. Achary, H.P. Sachin, Y.A. Naik, T.V. Venkatesha, The corrosion inhibition of mild steel by 3-formyl-8-hydroxy quinoline in hydrochloric acid medium, Mater. Chem. Phys. 107 (1) (2008) 44–50.
[6] P. Okafor, X. Liu, Y. Zheng, Corrosion inhibition of mild steel by ethylamino imidazoline derivative in CO2-saturated solution, Corros. Sci. 51 (4) (2009) 761–768.
[7] A. Popova, M. Christov, S. Raicheva, E. Sokolova, Adsorption and inhibitive properties of benzimidazole derivatives in acid mild steel corrosion, Corros. Sci. 46 (6) (2004) 1333–1350.
[8] H. Soliman, Influence of 8-hydroxyquinoline addition on the corrosion behavior of commercial Al and Al-HO411 alloys in NaOH aqueous media, Corros. Sci. 53 (9) (2011) 2994–3006.
[9] S. Shen, Y. Zuo, X. Zhao, The effects of 8-hydroxyquinoline on corrosion performance of a Mg-rich coating on AZ91D magnesium alloy, Corros. Sci. 76 (2013) 275–283.
[10] L. Tang, X. Li, Y. Si, G. Mu, G. Liu, The synergistic inhibition between 8-hydroxyquinoline and chloride ion for the corrosion of cold rolled steel in 0.5 M sulfuric acid, Mater. Chem. Phys. 95 (1) (2006) 29–38.
[11] H. Gao, Q. Li, Y. Dai, F. Luo, H. Zhang, High efficiency corrosion inhibitor 8-hydroxyquinoline and its synergistic effect with sodium dodecylbenzenesulphonate on AZ91D magnesium alloy, Corros. Sci. 52 (5) (2010) 1603–1609.
[12] I. Kartsonakis, I. Daniilidis, G. Kordas, Encapsulation of the corrosion inhibitor 8-hydroxyquinoline into ceria nanocontainers, J. Sol-Gel Sci. Technol. 48 (1–2) (2008) 24–31.
[13] A.C. Balaskas, I.A. Kartsonakis, L.A. Tziveleka, G.C. Kordas, Improvement of anticorrosive properties of epoxy-coated AA 2024–T3 with TiO2 nanocontainers loaded with 8-hydroxyquinoline, Prog. Org. Coat. 74 (3) (2012) 418–426.
[14] V.V. Gite, P.D. Tatiya, R.J. Marathe, P.P. Mahulikar, D.G. Hundiwale, Microencapsulation of quinoline as a corrosion inhibitor in polyurea microcapsules for application in anticorrosive PU coatings, Prog. Org. Coat. 83 (2015) 11–18.
[15] R. Kandyala, S.P.C. Raghavendra, S.T. Rajasekharan, Xylene: an overview of its health hazards and preventive measures, J. Oral Maxillofacial Pathol. JOMFP 14 (1) (2010) 1–5.
[16] L. Fishbein, An, overview of environmental and toxicological aspects of aromatic hydrocarbons II, Toluene. Sci. Total Environ. 42 (3) (1985) 267–288.
[17] S. Ma, Q. Ye, X. Pei, D. Wang, F. Zhou, Antifouling on gecko's feet inspired fibrillar surfaces: evolving from land to marine and from liquid repellency to algae resistance, Adv. Mater. Interfaces 2 (13) (2015) pp.
[18] D.M. Yebra, S. Kiil, K. Dam-Johansen, Antifouling technology—past, present and future steps towards efficient and environmentally friendly antifouling coatings, Prog. Org. Coat. 50 (2) (2004) 75–104.
[19] M. Lejars, A. Margaillan, C. Bressy, Fouling release coatings: a nontoxic alternative to biocidal antifouling coatings, Chem. Rev. 112 (8) (2012) 4347–4390.
[20] S. Cao, J. Wang, H. Chen, D. Chen, Progress of marine biofouling and antifouling technologies, Chin. Sci. Bull. 56 (7) (2011) 598–612.
[21] A. Tiraferri, Y. Kang, E.P. Giannelis, M. Elimelech, Superhydrophilic thin-film composite forward osmosis membranes for organic fouling control: fouling behavior and antifouling mechanisms, Environ. Sci. Technol. 46 (20) (2012) 11135–11144.
[22] J.E. Landmeyer, T.L. Tanner, B.E. Watt, Biotransformation of tributyltin to tin in freshwater river-bed sediments contaminated by an organotin release, Environ. Sci. Technol. 38 (15) (2004) 4106–4112.
[23] L. Chen, D.W. Au, C. Hu, D.R. Peterson, B. Zhou, P.-Y. Qian, Identification of molecular targets for 4, 5-dichloro-2-n-octyl-4-isothiazolin-3-one (DCOIT) in teleosts: new insight into mechanism of toxicity, Environ. Sci. Technol. 51 (3) (2017) 1840–1847.
[24] K.M. Almond, L.D. Trombetta, The effects of copper pyrithione, an antifouling agent, on developing zebrafish embryos, Ecotoxicology 25 (2) (2016) 389–398.

[25] J. Bellas, Comparative toxicity of alternative antifouling biocides on embryos and larvae of marine invertebrates, Sci. Total Environ. 367 (2–3) (2006) 573–585.
[26] J.R. Calo, P.G. Crandall, C.A. O'Bryan, S.C. Ricke, Essential oils as antimicrobials in food systems–A review, Food Control 54 (2015) 111–119.
[27] J. Reichling, P. Schnitzler, U. Suschke, R. Saller, Essential oils of aromatic plants with antibacterial, antifungal, antiviral, and cytotoxic properties – an Overview, Res. Complement. Med. 16 (2) (2009) 79–90.
[28] YB. Chong, H. Zhang, C.Y. Yue, J. Yang, Fabrication and release behavior of microcapsules with double-layered shell containing clove oil for antibacterial applications, ACS Appl. Mater. Interfaces (2018).
[29] L.B. Bullerman, F.Y. Lieu, S.A. Seier, Inhibition of growth and aflatoxin production by cinnamon and clove oils. cinnamic aldehyde and eugenol, J. Food Sci. 42 (4) (1977) 1107–1109.
[30] A.E. Edris, Pharmaceutical and therapeutic Potentials of essential oils and their individual volatile constituents: a review, Phytother. Res. 21 (4) (2007) 308–323.
[31] L.M. Meng, Y.C. Yuan, M.Z. Rong, M.Q. Zhang, A dual mechanism single-component self-healing strategy for polymers, J. Mater. Chem. 20 (29) (2010) 6030–6038.
[32] M. Keller, N. Sottos, Mechanical properties of microcapsules used in a self-healing polymer, Exp. Mech. 46 (6) (2006) 725–733.
[33] H.Y. Lee, S.J. Lee, I.W. Cheong, J.H. Kim, Microencapsulation of fragrant oil via in situ polymerization: effects of pH and melamine-formaldehyde molar ratio, J. Microencapsul 19 (5) (2002) 559–669.
[34] J. Yang, M.W. Keller, J.S. Moore, S.R. White, N.R. Sottos, Microencapsulation of isocyanates for self-healing polymers, Macromolecules 41 (24) (2008) 9650–9655.
[35] H. Zhang, P. Wang, J. Yang, Self-healing epoxy via epoxy–amine chemistry in dual hollow glass bubbles, Compos. Sci. Technol. 94 (2014) 23–29.
[36] M. Kanagasabhapathy, H. Sasaki, S. Haldar, S. Yamasaki, S. Nagata, Antibacterial activities of marine epibiotic bacteria isolated from brown algae of Japan, Ann. Microbiol. 56 (2) (2006) 167.
[37] N.E. Kimes, et al., Temperature regulation of virulence factors in the pathogen Vibrio coralliilyticus, ISME J. 6 (4) (2012) 835–846.
[38] S. Oyedemi, A. Okoh, L. Mabinya, G. Pirochenva, A. Afolayan, The proposed mechanism of bactericidal action of eugenol,∝-terpineol and g-terpinene against Listeria monocytogenes, Streptococcus pyogenes, Proteus vulgaris and Escherichia coli, Afr. J. Biotechnol. 8 (7) (2009) pp.
[39] S. Hemaiswarya, M. Doble, Synergistic interaction of eugenol with antibiotics against Gram negative bacteria, Phytomedicine 16 (11) (2009) 997–1005.
[40] A. Gill, R. Holley, Inhibition of membrane bound ATPases of escherichia coli and listeria monocytogenes by plant oil aromatics, Int. J. Food Microbiol. 111 (2) (2006) 170–174.
[41] S. Srisung et al., Antimicrobial activity of 8-hydroxyquinoline and transition metal complexes, 2013.
[42] J. Aljourani, K. Raeissi, M.A. Golozar, Benzimidazole and its derivatives as corrosion inhibitors for mild steel in 1M HCl solution, Corros. Sci. 51 (8) (2009/08/01/ 2009.) 1836–1843.
[43] Q. Wang, Y. Zhang, T. Hu, X. Jing, C. Meng, In situ preparation and optical properties of metal-8-hydroxyquinoline decoration of layered silicate: Self-assembly in the magadiite interface by solid-solid reaction, Microporous Mesoporous Mater. 246 (2017) 102–113.
[44] R.G. Charles, H. Freiser, R. Friedel, L.E. Hilliard, W.D. Johnston, Infra-red absorption spectra of metal chelates derived from 8-hydroxyquinoline, 2-methyl-8-hydroxyquinoline, and 4-methyl-8-hydroxyquinoline, Spectrochim. Acta 8 (1) (1956) 1–8.